ISSN: 2277-9655
Scientific Journal Impact Factor: 3.449
(ISRA), Impact Factor: 2.114

IJESRT

INTERNATIONAL JOURNAL OF ENGINEERING SCIENCES & RESEARCH TECHNOLOGY

LAPLACE TRANSFORM CALCULATION OF DARK SATURATION CURRENT IN SILICON SOLAR CELL INVOLVING EXCITONS EFFECTS

Mamadou Niane*, Omar.A.Niasse,Moulaye Diagne, Nacire Mbengue, Bassirou Ba

*Laboratoire de semiconducteurs et d'energie solaire,Departement de physique, Faculté des sciences et techniques(UCAD-SENEGAL)

Laboratoire de semiconducteurs et d'energie solaire,Departement de physique, Faculté des sciences et techniques(UCAD-SENEGAL)

ABSTRACT

In this work, the resolution of the differential equation system governing the electrons and excitons densities in the base region of a silicon solar cell is derived, using the Laplace transform. To check the validity of this method, a comparative study is made between the present results for the saturation current density and those obtained by R. Corkish and al in similar conditions with the same cell parameters. Numerical simulations for a silicon solar cell in the dark without polarization allows to obtain the excess minority carriers and excitons densities, the saturation current density according to various parameters of the cell such as the depth of the base, the doping level, the binding coefficient between electron and exciton, the lifetime and the recombination velocity etc....

Keywords: Saturation current, Laplace transform, exciton, binding coefficient

INTRODUCTION

Most of equations describing physical phenomena are of differential type. The resolution of these equations requires mathematical methods with appropriate boundary and initial conditions. The excitons transport in solar cells is governed by complex differential equations of which the resolution is tedious [1], [2], [3]. The method used in this paper to find numerical solutions for electrons and excitons densities is based on Laplace transform. The numerical simulations applied in a silicon solar cell in dark without polarization make possible to obtain profiles of the saturation current density according to the various parameters of the cell.

THEORY

Assumptions

In this study, some assumptions are made:

(1) Low-level injection is assumed.
(2) The depletion approximation
(3) Minority carriers in bulk regions are assumed to flow predominantly by diffusion.
(4) Within the depletion region the drift and diffusion currents are opposing and approximately equal in magnitude.
(5) Recombination in the depletion region is neglected.

Theorical calculation

The continuity equations governing the electrons density and the excitons by taking into account the binding of carriers pairs into excitons are as follows [4]:

$$\frac{1}{q}\Delta J_e = U_{eh} - G_{eh} + B \qquad (1)$$

$$\Delta\Phi = -U_x + G_x + B \qquad (2)$$

For cell in the dark (G_{eh}= 0 and G_x= 0)

The recombination terms can be simply expressed in terms of lifetimes:

$$U_{eh} = \frac{\Delta n}{\tau_e} \qquad (3)$$

and

$$U_x = \frac{\Delta n}{\tau_x} \qquad (4)$$

ISSN: 2277-9655
Scientific Journal Impact Factor: 3.449
(ISRA), Impact Factor: 2.114

From the law of mass action, the binding rate is given by [5], [6]:

$B=b(np-n^{*}n_x)$ (5)

The differential equations are as follows:

$$D_e\frac{d^2\Delta n}{dx^2}=\frac{\Delta n}{\tau_e}+b\left(\Delta nN_A-\Delta n_x.n^*\right) \quad (6)$$

$$D_x\frac{d^2\Delta n_x}{dx^2}=\frac{\Delta n_x}{\tau_x}-b\left(\Delta nN_A-\Delta n_x.n^*\right) \quad (7)$$

Let us express the excitons density Δn_x according to the one for excess minority carriers in the base *n* starting from the equation (4).

$$\Delta n_x=\frac{1}{bn^*}\left(\frac{1}{\tau_e}+bN_A\right)\Delta n-\frac{D_e}{bn^*}\frac{d^2\Delta n}{dx^2} \quad (8)$$

By replacing n_x in equation (7), the following differential equation is obtained:

$$\left[\frac{D_eD_x}{bn^*}\right]\frac{d^4\Delta n}{dx^4}-\left[\frac{D_e}{bn^*}\left(bn^*+\frac{1}{\tau_x}\right)+\frac{D_x}{bn^*}\left(bN_A+\frac{1}{\tau_e}\right)\right]\frac{d^2\Delta n}{dx^2}$$

$$+\left[\frac{1}{\tau_x}\left(\frac{N_A}{n^*}+\frac{1}{bn^*\tau_e}\right)+\frac{1}{\tau_e}\right]\Delta n=0 \quad (9)$$

Expression for excess minority carriers density

In order to simplify our preceding differential equation, let us pose:

$$A_1=\frac{D_eD_x}{bn^*} \quad (10)$$

$$A_2=\left[\frac{D_e}{bn^*}\left(bn^*+\frac{1}{\tau_x}\right)+\frac{D_x}{bn^*}\left(bN_A+\frac{1}{\tau_e}\right)\right] \quad (11)$$

$$A_3=\left[\frac{1}{\tau_x}\left(\frac{N_A}{n^*}+\frac{1}{bn\tau_e}\right)+\frac{1}{\tau_e}\right] \quad (12)$$

The differential equation (7) in simplified form becomes:

$$A_1\frac{d^4\Delta n}{dx^4}-A_2\frac{d^2\Delta n}{dx^2}+A_3\Delta n=0$$

(13)

The Laplace transform of equation (13) gives:

$$\Delta N(P)=\frac{A_2\sum_0^1 P^K\Delta n^{1-K}-A_1\sum_0^3 P^{3-K}\Delta n^K}{A_1P^4-A_2P^2+A_3} \quad (14)$$

Δn_o^k is the kth-derivatives of the density of the minority carriers in the base. Some of these values will be fixed and the others will be determined from boundary conditions [7].

$\Delta n_{oe}=10^{12}cm^{-3}$

The first derivative of the density of the excess minority carriers in the base is calculated starting from the boundary conditions [8].

$$\Delta n^{(1)}{}_{oe}=S_f\frac{\Delta n_{oe}}{D_e} \quad (15)$$

$$\Delta n^{(2)}{}_{oe}=10^{20}cm^{-5}$$

The 3rd derivative $\Delta n^{(3)}{}_{oe}$ has no influence on the saturation current density profiles; it can be considered as zero.

The final expression obtained is equivalent to this:

$$\Delta Nep(P)=\frac{-B_1P^3-B_2P^2+B_3P+B_4}{A_1P^4-A_2P^2+A_3} \quad (16)$$

with

$$B_1=A_1\Delta n_{oe} \quad (17)$$

$$B_2=A_1\Delta n_{oe}{}^{(2)} \quad (18)$$

$$B_3=A_2\Delta n_{0e}-A_1\Delta n^{(2)}{}_{oe} \quad (19)$$

$$B_4=A_2\Delta n^{(1)}{}_{oe}-A_1\Delta n^{(3)}{}_{oe} \quad (20)$$

Let us determine the values α_1, α_2, α_3, α_4, α_5, α_6 and α_7 so that:

$$\Delta N(P)=\frac{\alpha_1P+\alpha_2}{\alpha_3P^2+\alpha_4}+\frac{\alpha_5P+\alpha_6}{\alpha_3P^2+\alpha_7} \quad (21)$$

After calculation, we obtain differentials expressions of the constants α_i(see appendix)

The expression for excess minority carriers density as a function of the base depth ($0\le x\le H$) is

$$\Delta n=\frac{\alpha_1}{\alpha_3}\cosh(\beta_1x)+\frac{\alpha_2}{\alpha_3\beta_1}\sinh(\beta_1x)$$

$$+\frac{\alpha_5}{\alpha_3}\cosh(\beta_2x)+\frac{\alpha_6}{\alpha_3\beta_2}\sinh(\beta_2x) \quad (22)$$

I.1. Expression of the excitons density

The excitons density expression in the dark is deduced from equation (8):

ISSN: 2277-9655
Scientific Journal Impact Factor: 3.449
(ISRA), Impact Factor: 2.114

After calculation, the following expression is obtained:

$$\Delta n_x =$$
$$\left[\frac{\alpha_1}{\alpha_3 bn^*}\left(bN_A+\frac{1}{\tau_e}\right)-\frac{D_e(\beta_1)^2\alpha_1}{bn^*\alpha_3}\right]\cosh(\beta_1 x)$$
$$+\left[\frac{\alpha_2}{\alpha_3\beta_1 bn^*}\left(bN_A+\frac{1}{\tau_e}\right)-\frac{D_e\beta_1\alpha_2}{bn^*\alpha_3}\right]\sinh(\beta_1 x)$$
$$+\left[\frac{\alpha_5}{\alpha_3 bn^*}\left(bN_A+\frac{1}{\tau_e}\right)-\frac{D_e(\beta_2)^2\alpha_5}{bn^*\alpha_3}\right]\cosh(\beta_2 x)$$
$$+\left[\frac{\alpha_6}{\alpha_3\beta_2 bn^*}\left(bN_A+\frac{1}{\tau_e}\right)-\frac{D_e\beta_2\alpha_6}{bn^*\alpha_3}\right]\sinh(\beta_2 x) \qquad (23)$$

Expression of the current density

Assuming that electrons and excitons transports in the base are largely dominated by the diffusion, the expression of the current density according to the depth of the base, the binding coefficient and the doping level becomes as follows:

$$J = qD_e\frac{d}{dx}\Delta n + qD_x\frac{d}{dx}\Delta n_x \qquad (24)$$

$$J(x)=$$
$$\left[qD_e\frac{\alpha_1\beta_1}{\alpha_3}+qD_x\left[\frac{\alpha_1\beta_1}{\alpha_3 bn^*}\left(bN_A+\frac{1}{\tau_e}\right)-\frac{D_e(\beta_1)^3\alpha_1}{bn^*\alpha_3}\right]\right]\sinh(\beta_1 x)$$
$$+\left[qD_e\frac{\alpha_2}{\alpha_3}+qD_x\left[\frac{\alpha_2}{\alpha_3 bn^*}\left(bN_A+\frac{1}{\tau_e}\right)-\frac{D_e(\beta_1)^2\alpha_2}{bn^*\alpha_3}\right]\right]\cosh(\beta_1 x)$$
$$+\left[qD_e\frac{\alpha_5\beta_2}{\alpha_3}+qD_x\left[\frac{\alpha_5\beta_2}{\alpha_3 bn^*}\left(bN_A+\frac{1}{\tau_e}\right)-\frac{D_e(\beta_2)^3\alpha_5}{bn^*\alpha_3}\right]\right]\sinh(\beta_2 x)$$
$$+\left[qD_e\frac{\alpha_6}{\alpha_3}+qD_x\left[\frac{\alpha_6}{\alpha_3 bn^*}\left(bN_A+\frac{1}{\tau_e}\right)-\frac{D_e(\beta_2)^2\alpha_6}{bn^*\alpha_3}\right]\right]\cosh(\beta_2 x)$$

(25)

The expression of the saturation current density in the junction is obtained by considering x = 0 in equation (25).

$$J_0 = qD_e\left(\frac{\alpha_2+\alpha_6}{\alpha_3}\right)+qD_x\left\{\begin{array}{l}\left(\frac{\alpha_2+\alpha_6}{\alpha_3 bn^*}\right)\left(bN_A+\frac{1}{\tau_e}\right)\\ -\frac{D_e}{bn^*\alpha_3}\left((\beta_2)^2\alpha_6+(\beta_1)^2\alpha_2\right)\end{array}\right\} \qquad (26)$$

Comparisons will be made with the one given in [4].

$$J_0' = -\frac{1}{2}qD_e\left\{\begin{array}{l}\varepsilon_+^{\frac{1}{2}}\left[1+(M_\Delta+2rM_{21})\delta^{-\frac{1}{2}}\right]\\ +\varepsilon_-^{\frac{1}{2}}\left[1-(M_\Delta+2rM_{21})\delta^{-\frac{1}{2}}\right]\end{array}\right\}n_{oe} \qquad (27)$$

Comparative study

In fig. 1, the variation of the current density profile is represented with the binding coefficient.

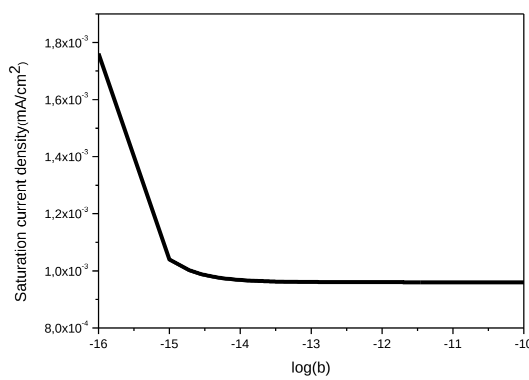

Fig.1. Saturation current density in function to the logarithm of the binding coefficient ($N_A = 10^{18}\ cm^{-3}$, H = 100 nm, Sf=310 ^{3} cm/s $\Delta n_{oe} = 10^{12}\ cm^{-3}$, $\Delta n_{oe}^{(2)} = 10^{20}\ cm^{-5}$, $D_e = 13\ cm^2/s$, $D_x = 26 cm^2/s$)

The comparisons between this density profile and the one obtained from Corkish [4] in the same conditions and using the same parameters of the cell are displayed in figure(2):

ISSN: 2277-9655
Scientific Journal Impact Factor: 3.449
(ISRA), Impact Factor: 2.114

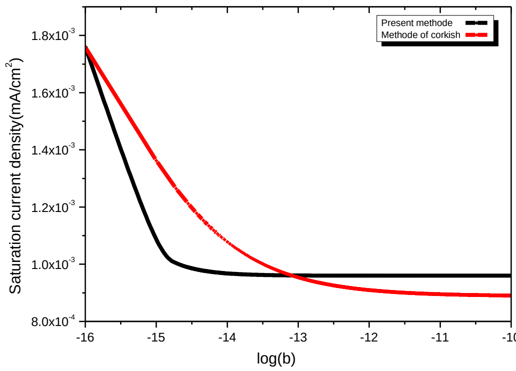

Fig. 2. Saturation current density in function to the logarithm of the binding coefficient ($N_A = 10^{18}$ cm^{-3}, H = 100 nm, $S_f = 310^3$ cm/s, $\Delta n_{oe} = 10^{12}$ cm^{-3}, $\Delta n_{oe}^{(2)} = 10^{20}$ cm^{-5}, $D_e = 13$ cm²/s, $D_x = 26$cm²/s)

The comparison of the profiles shows a similar decrease of two the saturation current density according to the binding coefficient b.

An increase in this coefficient b causes strong volume recombination which reduces the density of the excess minority carriers in the base. Accordingly, a reduction in the current density is observed for these two profiles when the coupling becomes increasingly strong [9], [10].

The difference noted between the curves comes from the parameters $\Delta n_{oe}^{(2)}$and $\Delta n_{oe}^{(3)}$which respectively represent the second and third derivatives of the excess minority carriers the density at the junction given by the boundary conditions. This difference could be due to the fact that the derivatives of the density of the electrons to the junction should depend on the nature of the coupling.

RESULTS AND DISCUSSION

From the present work, the current density can be examined as a function of binding coefficient through various cell parameters as doping level.

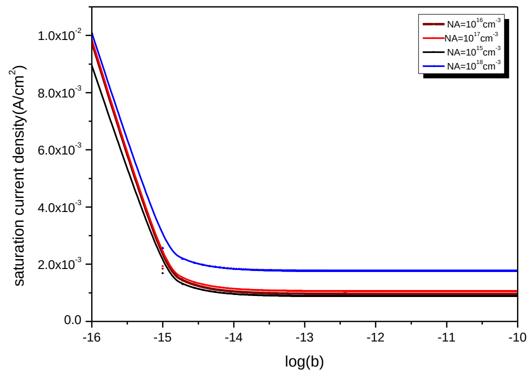

Fig. 3. Saturation current density in function to the logarithm of the binding coefficient for different doping level (H = 100 nm, Sf= 3.10^3 cm/s, $\Delta n_{oe} = 10^{12}$ cm^{-3}, $\Delta n_{oe}^{(2)} = 10^{20}$ cm^{-5} ,D_e=13 cm²/s,D_x= 26cm²/s)

The analysis of profiles density shows three parts with a first one corresponding to a very weak coupling (b=10^{-15} $cm^3.s^{-1}$) or a very significant decrease of the current density with the binding coefficient. The second part for which $10^{-15} cm^3.s^{-1} \leq b \leq 10^{-13.6}$ $cm^3.s^{-1}$ is characterized by a weak variation of current density. The third part, corresponding to a strong coupling (b $\geq 10^{-13.5}$ $cm^3.s^{-1}$), is characterized by a constant value of the saturation current density for each doping level. This is very comprehensible because for a strong coupling the rate of recombination reaches its maximum value. Thus, current density does not vary any more according to the binding coefficient making constant the excess minority carriers density and consequently that of the current. On the other hand, when the coupling is weak, the rate of recombination strongly increases and involves the reduction of the minority carriers density in the base [11].

ISSN: 2277-9655
Scientific Journal Impact Factor: 3.449
(ISRA), Impact Factor: 2.114

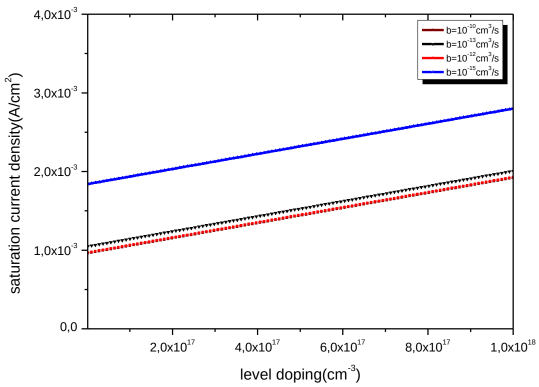

Fig. 4. Saturation current density in the base in function to the doping level for different values of the binding coefficient (H = 100nm, Sf= 3.10 ^{3} cm/s, Δn_{oe}= 10 ^{12} cm $^{-3}$, $\Delta n_{oe}^{(2)}$= 10 ^{20} cm $^{-5}$, D_e = 13 cm²/s, D_x= 26cm²/s)

Figure 4 shows a linear variation of the saturation current density according to the level doping for different values of binding coefficient. The same slope is obtained for any values of binding coefficient. It can be noted that when the coupling is strong ($b>10^{-13.4}cm^3.s^{-1}$), the saturation current density profile is the same whatever the values of the binding coefficient in this interval, this confirms well the analyses made above because when the coupling is strong and the minority carriers density reaches its limit value. For weak coupling ($b \leq 10^{-14}$ $cm^3.s^{-1}$), an increase of saturation current density is observed; this is simply due to a variation of the recombination rate at the junction. Indeed, the volume recombination caused by a strong coupling is reduced for small values of coefficient b. Consequently a significant increase in the density of the excess minority carriers implies the reduction of the saturation current density [12], [13].

CONCLUSION

The use of Laplace transform in the resolution of the differential equations system governing the excess minority carriers and excitons density in the base of a silicon solar cell, allows having a better knowledge on the influence of excitons on the current density in the base. It is a very simple method of resolution compared to that used byR. Corkish and al. which requires more thorough in algebra. This method enables to define two additional parameters in the base which are the second and third derivative of the density of the excess minority carriers to the junction. Thus for a good understand of these two parameters, the studies on their variation for different parameters of the solar cell and different boundary conditions could be carried out.

Appendix

Determination of the α_I coefficient from equations (16). The transformation of Laplace of the of the excess minority carriers in the base is given the following expression:

$$\Delta Nep(P) = \frac{-B_1P^3 - B_2P^2 + B_3P + B_4}{A_1P^4 - A_2P^2 + A_3}$$

Let us determine then expressions α_1 α_2 , α_3 , α_4 α_5 α_6 α_7 such as

$$\Delta Nep(P) = \frac{\alpha_1 P + \alpha_2}{\alpha_3 P^2 + \alpha_4} + \frac{\alpha_5 P + \alpha_6}{\alpha_3 P^2 + \alpha_7} \quad (A1)$$

We thus obtain the equality according to:

$$\frac{\alpha_1 P + \alpha_2}{\alpha_3 P^2 + \alpha_4} + \frac{\alpha_5 P + \alpha_6}{\alpha_3 P^2 + \alpha_7} = \frac{-B_1P^3 - B_2P^2 + B_3P + B_4}{A_1P^4 - A_2P^2 + A_3} \quad (A2)$$

By identification we obtain the system of equation following:

$$\begin{cases} {\alpha_3}^2 = A_1 \\ \alpha_3\alpha_7 + \alpha_3\alpha_4 = -A_2 \\ \alpha_4\alpha_7 = A_3 \\ \alpha_1\alpha_3 + \alpha_3\alpha_5 = -B_1 \\ \alpha_2\alpha_3 + \alpha_3\alpha_6 = -B_2 \\ \alpha_1\alpha_7 + \alpha_5\alpha_4 = B_3 \\ \alpha_2\alpha_7 + \alpha_4\alpha_6 = B_4 \end{cases} \quad (A3)$$

The resolution of this system gives the following expressions of α_I according to the parameters of cell.

$$\alpha_3\left(b,N_A\right)=\sqrt{\frac{D_eD_x}{bn^*}} \qquad \text{(A4)}$$

$$\alpha_4\left(b,N_A\right)=-\frac{1}{2}\left[\frac{\frac{D_e}{bn^*}\left(bn^*+\frac{1}{\tau_x}\right)+\frac{D_x}{bn^*}\left(bN_A+\frac{1}{\tau_e}\right)}{\sqrt{\frac{D_eD_x}{bn^*}}}\right]\left[1+\sqrt{1-\frac{4.\frac{D_eD_x}{bn^*}\left[\frac{1}{\tau_x}\left(\frac{N_A}{n^*}+\frac{1}{bn\tau_e}\right)+\frac{1}{\tau_e}\right]}{\left[\frac{D_e}{bn^*}\left(bn^*+\frac{1}{\tau_x}\right)+\frac{D_x}{bn^*}\left(bN_A+\frac{1}{\tau_e}\right)\right]^2}}\right] \qquad \text{(A5)}$$

$$\alpha_7\left(b,N_A\right)=\frac{1}{2}\left[\frac{\frac{D_e}{bn^*}\left(bn^*+\frac{1}{\tau_x}\right)+\frac{D_x}{bn^*}\left(bN_A+\frac{1}{\tau_e}\right)}{\sqrt{\frac{D_eD_x}{bn^*}}}\right]\left[-1+\sqrt{1-\frac{4.\frac{D_eD_x}{bn^*}\left[\frac{1}{\tau_x}\left(\frac{N_A}{n^*}+\frac{1}{bn\tau_e}\right)+\frac{1}{\tau_e}\right]}{\left[\frac{D_e}{bn^*}\left(bn^*+\frac{1}{\tau_x}\right)+\frac{D_x}{bn^*}\left(bN_A+\frac{1}{\tau_e}\right)\right]^2}}\right] \qquad \text{(A6)}$$

$$\alpha_6\left(b,N_A\right)=\frac{\frac{\Delta n^*_{0e}\left(\frac{D_eD_x}{bn^*}\right)^{\frac{3}{2}}}{\frac{D_e}{bn^*}\left(bn^*+\frac{1}{\tau_x}\right)+\frac{D_x}{bn^*}\left(bN_A+\frac{1}{\tau_e}\right)}-\frac{1}{2}\Delta n_{0e}\sqrt{\frac{D_eD_x}{bn^*}}\left[1+\sqrt{1-\frac{4.\frac{D_eD_x}{bn^*}\left[\frac{1}{\tau_x}\left(\frac{N_A}{n^*}+\frac{1}{bn\tau_e}\right)+\frac{1}{\tau_e}\right]}{\left[\frac{D_e}{bn^*}\left(bn^*+\frac{1}{\tau_x}\right)+\frac{D_x}{bn^*}\left(bN_A+\frac{1}{\tau_e}\right)\right]^2}}\right]}{\sqrt{1-\frac{4\frac{D_eD_x}{bn^*}\left[\frac{1}{\tau_x}\left(\frac{N_A}{n^*}+\frac{1}{bn\tau_e}\right)+\frac{1}{\tau_e}\right]}{\left[\frac{D_e}{bn^*}\left(bn^*+\frac{1}{\tau_x}\right)+\frac{D_x}{bn^*}\left(bN_A+\frac{1}{\tau_e}\right)\right]^2}}} \qquad \text{(A7)}$$

$$\alpha_2\left(b,N_A\right)=\frac{\frac{-\Delta n^*_{0e}\left(\frac{D_eD_x}{bn^*}\right)^{\frac{3}{2}}}{\frac{D_e}{bn^*}\left(bn^*+\frac{1}{\tau_x}\right)+\frac{D_x}{bn^*}\left(bN_A+\frac{1}{\tau_e}\right)}+\frac{1}{2}\Delta n_{0e}\sqrt{\frac{D_eD_x}{bn^*}}\left[1-\sqrt{1-\frac{4.\frac{D_eD_x}{bn^*}\left[\frac{1}{\tau_x}\left(\frac{N_A}{n^*}+\frac{1}{bn\tau_e}\right)+\frac{1}{\tau_e}\right]}{\left[\frac{D_e}{bn^*}\left(bn^*+\frac{1}{\tau_x}\right)+\frac{D_x}{bn^*}\left(bN_A+\frac{1}{\tau_e}\right)\right]^2}}\right]}{\sqrt{1-\frac{4\frac{D_eD_x}{bn^*}\left[\frac{1}{\tau_x}\left(\frac{N_A}{n^*}+\frac{1}{bn\tau_e}\right)+\frac{1}{\tau_e}\right]}{\left[\frac{D_e}{bn^*}\left(bn^*+\frac{1}{\tau_x}\right)+\frac{D_x}{bn^*}\left(bN_A+\frac{1}{\tau_e}\right)\right]^2}}} \qquad \text{(A8)}$$

$$\alpha_1\left(b,N_A\right)=\frac{\frac{\Delta n^*_{0e}\left(\frac{D_eD_x}{bn^*}\right)^{\frac{3}{2}}}{\frac{D_e}{bn^*}\left(bn^*+\frac{1}{\tau_x}\right)+\frac{D_x}{bn^*}\left(bN_A+\frac{1}{\tau_e}\right)}-\frac{1}{2}\Delta n_{0e}\sqrt{\frac{D_eD_x}{bn^*}}\left[1+\sqrt{1-\frac{4.\frac{D_eD_x}{bn^*}\left[\frac{1}{\tau_x}\left(\frac{N_A}{n^*}+\frac{1}{bn\tau_e}\right)+\frac{1}{\tau_e}\right]}{\left[\frac{D_e}{bn^*}\left(bn^*+\frac{1}{\tau_x}\right)+\frac{D_x}{bn^*}\left(bN_A+\frac{1}{\tau_e}\right)\right]^2}}\right]}{\sqrt{1-\frac{4\frac{D_eD_x}{bn^*}\left[\frac{1}{\tau_x}\left(\frac{N_A}{n^*}+\frac{1}{bn\tau_e}\right)+\frac{1}{\tau_e}\right]}{\left[\frac{D_e}{bn^*}\left(bn^*+\frac{1}{\tau_x}\right)+\frac{D_x}{bn^*}\left(bN_A+\frac{1}{\tau_e}\right)\right]^2}}} \qquad \text{(A9)}$$

$$\alpha_5\left(b,N_A\right)=\frac{\frac{\Delta n^*_{0e}\left(\frac{D_eD_x}{bn^*}\right)^{\frac{3}{2}}}{\frac{D_e}{bn^*}\left(bn^*+\frac{1}{\tau_x}\right)+\frac{D_x}{bn^*}\left(bN_A+\frac{1}{\tau_e}\right)}-\frac{1}{2}\Delta n_{0e}\sqrt{\frac{D_eD_x}{bn^*}}\left[1+\sqrt{1-\frac{4.\frac{D_eD_x}{bn^*}\left[\frac{1}{\tau_x}\left(\frac{N_A}{n^*}+\frac{1}{bn\tau_e}\right)+\frac{1}{\tau_e}\right]}{\left[\frac{D_e}{bn^*}\left(bn^*+\frac{1}{\tau_x}\right)+\frac{D_x}{bn^*}\left(bN_A+\frac{1}{\tau_e}\right)\right]^2}}\right]}{\sqrt{1-\frac{4\frac{D_eD_x}{bn^*}\left[\frac{1}{\tau_x}\left(\frac{N_A}{n^*}+\frac{1}{bn\tau_e}\right)+\frac{1}{\tau_e}\right]}{\left[\frac{D_e}{bn^*}\left(bn^*+\frac{1}{\tau_x}\right)+\frac{D_x}{bn^*}\left(bN_A+\frac{1}{\tau_e}\right)\right]^2}}} \qquad \text{(A10)}$$

$$\beta_1=\sqrt{-\frac{\alpha_4}{\alpha_3}} \qquad \text{(A11)}$$

And

$$\beta_2=\sqrt{-\frac{\alpha_7}{\alpha_3}} \qquad \text{(A12)}$$

we obtain theexpressions following

$$\beta_2\left(N_A,b\right)=\sqrt{\frac{1}{2}\left[\frac{\frac{D_e}{bn^*}\left(bn^*+\frac{1}{\tau_x}\right)+\frac{D_x}{bn^*}\left(bN_A+\frac{1}{\tau_e}\right)}{\frac{D_eD_x}{bn^*}}\right]\left[1-\sqrt{1-\frac{4\frac{D_eD_x}{bn^*}\left[\frac{1}{\tau_x}\left(\frac{N_A}{n^*}+\frac{1}{bn\tau_e}\right)+\frac{1}{\tau_e}\right]}{\left[\frac{D_e}{bn^*}\left(bn^*+\frac{1}{\tau_x}\right)+\frac{D_x}{bn^*}\left(bN_A+\frac{1}{\tau_e}\right)\right]^2}}\right]} \qquad \text{(A13)}$$

$$\beta_2\left(N_A,b\right)=\sqrt{\frac{1}{2}\left[\frac{\frac{D_e}{bn^*}\left(bn^*+\frac{1}{\tau_x}\right)+\frac{D_x}{bn^*}\left(bN_A+\frac{1}{\tau_e}\right)}{\frac{D_eD_x}{bn^*}}\right]\left[1+\sqrt{1-\frac{4\frac{D_eD_x}{bn^*}\left[\frac{1}{\tau_x}\left(\frac{N_A}{n^*}+\frac{1}{bn\tau_e}\right)+\frac{1}{\tau_e}\right]}{\left[\frac{D_e}{bn^*}\left(bn^*+\frac{1}{\tau_x}\right)+\frac{D_x}{bn^*}\left(bN_A+\frac{1}{\tau_e}\right)\right]^2}}\right]} \qquad \text{(A14)}$$

REFERENCES

[1] M. A. Green, Silicon Solar Cells. Advanced Principles and Practice Bridge, Sydney, 1995!, pp. 81–83

[2] J. Barrau, M. Heckmann, M. Brousseau, Determination experimentale du coefficient de formation d'excitons dans le siliciumJournal of Physics and Chemistry of Solids, 34, 3, 1973, 381-385

[3] D. E .Kane, R. M. Swanson, Effect of exciton on visible strip shrinking and transport of semiconductor , Journal of Applied Physics, vol.73 n.3, February 1993,pp.1193 – 1197

[4] R. Corkish, Daniel S-p. Chan and M. A. Green, "excitons in Silicon Diodes and Solar Cells - A Three Particle Theory", Journal of Applied Physics, vol. 79, pp. 195-203, 1996

[5] Yong Zhang , Angelo Mascarenhas , Satyen Deb , Effects of excitons on solar cells, Journal of Applied Physics, vol. 84n.7,octobre 1998, pp. 3966-3971

[6] Arthur J. Nozik, Multiple exciton generation in semiconductor quantum dots Chemical Physics Letters 457 (2008) 3–11

[7] Michael P. Stewart and Jillian M. Buriak "Exciton-Mediated Hydrosilylation on Photoluminescent Nanocrystalline Silicon" J. Am. Chem. Soc. 2001, 123, 7821-7830

[8] Matthew C Beard, Kelly P. Knutsen, Pingrong Yu, Joseph M. Luther, Qing Song, Wyatt K Metzger, Randy J Ellingsonand Arthur J Nozik. Multiple Exciton Generationin Colloidal Silicon NanocrystalsNANOLETTERS2007Vol. 7, No 8 2506 – 2512

[9] A. Richter[a],* , F. Werner[b], A. Cuevas[c], J. Schmidt[b], S.W. Glunz[a] Improved

ISSN: 2277-9655
Scientific Journal Impact Factor: 3.449
(ISRA), Impact Factor: 2.114

parameterization of Auger recombination in silicon, Energy Procedia 27 (2012) 88 – 94

[10] A. J Nozik, M. C Beard, J. Mr. Luther, M. Law, R. J Ellingson, and J C Johnson Semiconductor Quantum Dots and Quantum Dot Arrays and Applications of Multiple Exciton Generation to Third-Generation Photovoltaic Solar Cells dots Chemical Physics Letters. Rev. 2010, 110, 6873 –6890

[11] D.-J. Jang,[a]_ G.-T. Lin, C.-L. Hsiao,[b]_ and L. W. Tu"Auger recombination in InN thin films" APPLIED PHYSICS LETTERS92, 042101 _2008

[12] Marc Dvorak,[1] Su-Huai Wei,[2] and Zhigang Wu1,*" Origin of the Variation of Exciton Binding Energy in Semiconductors" PHYSICAL REVIEW LETTERS 110, 016402 (2013)

[13] Kerr MJ and Cuevas A. General parameterization of Auger recombination in crystalline silicon.JAppl. Phys. 2002; 91:2473-80